Cross Section Analysis of the Gas-Phase Potential Surface for the Addition of Water to Formaldehyde. A Theoretical Study of the Energetics of Proton Transfer as a Function of ΔpK_a

Shmaryahu Hoz,*,† Kiyull Yang,‡ and Saul Wolfe*

Contribution from the Department of Chemistry, Queen's University, Kingston, Ontario, Canada K7L 3N6. *Received August 9, 1988*

Abstract: The cyclic structure for the gas-phase addition of water to formaldehyde combines C–O bond formation and proton transfer. This structure and two different kinds of Jencks–More-O'Ferrall surfaces comprised of C–O bond formation and proton transfer, have been computed at both the semiempirical AM1 and ab initio 3-21G levels. As the C–O distance is shortened, the thermodynamic driving force for the proton-transfer reaction increases, and linear Brönsted plots ($\Delta E^{\ddagger}$ versus ΔE) result, with slopes 0.53–0.79 over a range of 55–80 kcal/mol in ΔE. Slopes calculated at the two different levels of theory are in good agreement. Despite the extended ranges of the linear Brönsted plots, the transition-state structures for the proton-transfer reactions vary significantly, and the BEMA HAPOTHLE principle is obeyed. Consequently, the slopes of the Brönsted plots cannot be used to estimate the degree of proton transfer at the transition state. Although, in general, the Marcus equation successfully predicts the activation energies and the variation in the transition-state structure, statistical analysis reveals that the accommodation of the data to the linear Brönsted equation is an order of magnitude better than the quadratic Marcus equation. Because the barriers for the proton-transfer reactions are significant, at the cyclic transition state ΔE ($\equiv\Delta pK_a$) between the proton donor and acceptor moieties is not zero, and a thermodynamic driving force of 30–40 kcal/mol is needed to achieve the proton jump.

Proton transfer plays an important role in the catalysis of nucleophilic additions to carbonyl groups and is often coupled to the nucleophilic step (general acid–general base catalysis). In the course of the uncatalyzed addition of water to formaldehyde, to form the unstable[1] zwitterionic adduct **1** (eq 1), the H_2O moiety acquires a positive charge and becomes more acidic; concurrently, the CH_2O moiety acquires a negative charge and becomes more basic. The existence of general base catalysis in such a reaction (eq 2) implies that proton transfer to B is endoergic on the side of the reactants and exoergic on the side of the products.[2] An analogous argument applies, in the case of general acid catalysis (eq 3), for proton transfer to oxygen. The actual proton jump is thought to occur, in a catalyzed process, at that point on the reaction coordinate where the pK_a's of the proton donor and B (eq 2) or the proton acceptor and A (eq 3) become equal.[3]

$$H_2O + CH_2O \longrightarrow \underset{\mathbf{1}}{H_2\overset{+}{O}-CH_2O^-} \quad (1)$$

$$B\ H-O(H)\ CH_2O \longrightarrow BH^+ + HO-CH_2-O^- \quad (2)$$

$$H-O(H)\ CH_2O\ H-A \longrightarrow H_2\overset{+}{O}-CH_2OH + A^- \quad (3)$$

The addition of water to formaldehyde in the gas phase via the cyclic transition structure **2** has been discussed by Williams and co-workers[4] and features intramolecular general acid and general base catalysis. Because of this feature, it is possible, from an analysis of the computed H_2O–CH_2O energy surface, to probe the proton jump hypothesis[3] in the gas phase and, more generally, to study the energetics of proton transfer as a function of ΔE ($\equiv\Delta pK_a$).

By using the semiempirical program AMPAC,[5] with the AM1 Hamiltonian,[6] **2** was located by a two-dimensional grid search followed by full geometry optimization with the SIGMA option. The fully optimized 3-21G structure[7] of **2** was also located by using, successively, the AM1 and STO-3G structures and force constants as starting points. The transition structures are, in each case, characterized by a single imaginary frequency whose transition vector is, as expected,[3,4] dominated by the motion of a hydrogen between the two oxygens (see **2**).

Figure 1 is the Jencks–More-O'Ferrall surface[8] for the reaction, calculated at the AM1 level. Each point on the grid used to generate this surface is characterized by its O^2–C (r) and O^2–H^1 distances and is fully optimized with respect to the 13 other parameters. The locations of the transition states for the proton-transfer reactions (motion from left to right across the potential surface) were further refined beyond the original grid resolution, and each of these structures was found to have only one negative eigenvalue in its second derivative matrix. This demonstration was especially necessary in the present case because the surface of Figure 1 is expected[9a] to be "double-valued" when the grid size

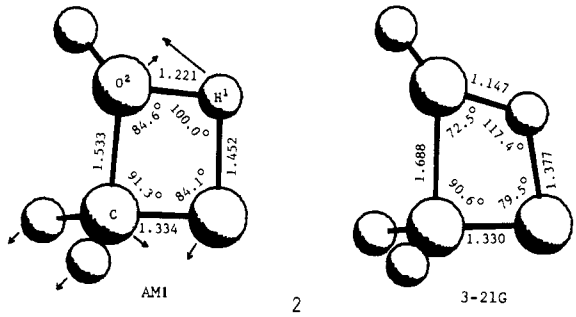

2

† On leave from Bar-Ilan University, Ramat Gan, Israel.
‡ Dedicated to Professor Ikchoon Lee on the occasion of his 60th birthday.

(1) Sörensen, P. E.; Jencks, W. P. *J. Am. Chem. Soc.* **1987**, *109*, 4675.
(2) Jencks, W. P. *Chem. Rev.* **1972**, *72*, 705.
(3) Guthrie, J. P. *J. Am. Chem. Soc.* **1980**, *102*, 5286.
(4) Williams, I. H.; Spangler, D.; Femec, D. A.; Maggiora, G. M.; Schowen, R. L. *J. Am. Chem. Soc.* **1980**, *102*, 6619. Williams, I. H.; Maggiora, G. M.; Schowen, R. L. *J. Am. Chem. Soc.* **1980**, *102*, 7831. Williams, I. H.; Spangler, D.; Maggiora, G. M.; Schowen, R. L. *J. Am. Chem. Soc.* **1985**, *107*, 7717.
(5) Available from Quantum Chemistry Program Exchange (QCPE). We authors thank Professor M. J. S. Dewar for a copy of the VAX version 2.10. This was converted to the VMS operating system of the Queen's University IBM 3081 computer.
(6) Dewar, M. J. S.; Zoebisch, E. G.; Healy, E. F.; Stewart, J. J. P. *J. Am. Chem. Soc.* **1985**, *107*, 3902.
(7) Binkley, J. S.; Pople, J. A.; Hehre, W. J. *J. Am. Chem. Soc.* **1980**, *102*, 939.
(8) More-O'Ferrall, R. A. *J. Chem. Soc. B* **1970**, 274. Jencks, D. A.; Jencks, W. P. *J. Am. Chem. Soc.* **1977**, *99*, 7948.

0002-7863/90/1512-1319$02.50/0

Table I. A Comparison of AM1 and 3-21G Reaction Energies[a] (ΔE) and Activation Energies[a] ($\Delta E^{\ddagger}$) for the Horizontal Cross Sections of the Theoretical Jencks-More-O'Ferrall Surfaces (r = C^2–O Distance)

	Brönsted plot a[b]				Brönsted plot b[c]			
	AM1		3-21G		AM1		3-21G	
r (Å)	ΔE	$\Delta E^{\ddagger}$	ΔE	$\Delta E^{\ddagger}$	ΔE	$\Delta E^{\ddagger}$	ΔE	$\Delta E^{\ddagger}$
2.20							76.53	105.28
2.00	36.33	55.29			49.92	75.74	51.96	82.30
1.90	21.09	46.08	13.97	30.02	35.64	67.21		
1.80	4.83	36.77	-3.48	20.57	20.04	58.25	19.77	56.15
1.70	-11.97	27.75	-25.66	11.97	3.54	47.37	1.47	43.03
1.68			-29.37	10.39			-4.26	40.39
1.65			-34.91	8.13				
1.60	-28.68	19.44	-40.18	4.71				
1.55	-36.83	15.70						
1.53	-39.87	14.41						
slope[d]	0.53		0.45		0.73		0.79	
$\Delta E_0^{\ddagger}$[e]	35.0		22.2		41.39		42.8	
$\Delta E^{\ddagger}$[f]	-39.5		-29.5					
$\Delta E^{\ddagger}$[g]	12.0		10.4					

[a] In kcal/mol. [b] All structures fully optimized ("coupled" surfaces). [c] Reactant geometry retained in the horizontal cross section ("uncoupled" surfaces: see text). [d] Slope of the Brönsted plot. [e] Intrinsic barrier in kcal/mol, i.e., the barrier for $\Delta E = 0$. [f] Energy difference between reactants and product in the cross section that passes through **2**. [g] Barrier connecting reactants and product in the cross section that passes through **2**.

for the horizontal motion is sufficiently small. Indeed, when the grid sizes were reduced from 0.1 to 0.01 Å in the regions of the maxima, the discontinuities described in ref 9a were observed. Since surface fitting to the lower of each such doublet of energies would be inappropriate, the actual surface shown in Figure 1 was produced by splining through fully characterized stationary points.

The 3-21G surface corresponding to Figure 1 (stationary points only) was also calculated.[9b]

Strong electronic and geometrical coupling is enforced in cyclic transition structures such as **2**. In such a case, even a small change in geometry can have a large effect upon the electronic distribution and, therefore, upon the energy, and bias the analysis of Figure 1 and its 3-21G counterpart. Accordingly, a second surface was generated at both AM1 and 3-21G levels, in which only the left-hand side (reactants) was optimized fully for each r. The transition states and the products of each horizontal cross section retained the geometry of the reactants, and only the position of the transferred proton was optimized. This strategy was expected to reduce coupling significantly.

The data summarized in Table I allow evaluation of a number of rate-equilibrium correlations: (i) the issues of linearity versus curvature in Brönsted plots, or in free energy relationships generally, and interpretations of the slopes of such plots have been the focus of many studies in physical organic chemistry.[10] Ex-

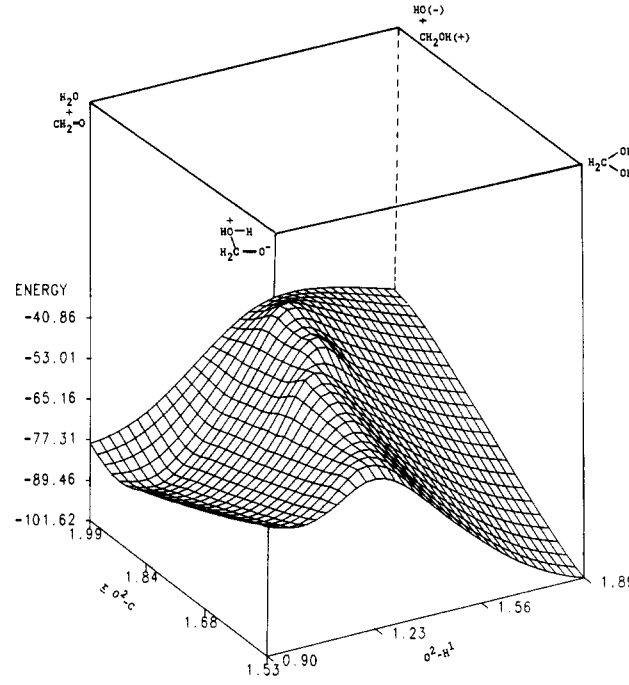

Figure 1. Jencks-More-O'Ferrall surface for the reaction of CH_2O with H_2O, computed at the AM1 level. Energy (kcal/mol) is shown as a function of O^2–C (r) and O^2–H^1 (see **2**).

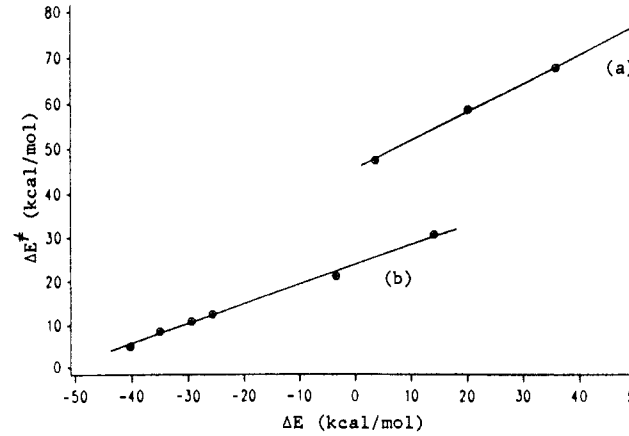

Figure 2. (a) Brönsted plot for the cross sections of the "uncoupled" surface computed at AM1. (b) Brönsted plot for the "coupled" (i.e., optimized) surface computed at 3-21G.

(9) (a) Williams, I. H.; Maggiora, G. M. *J. Mol. Struct. (THEOCHEM)* **1982**, *6*, 365. (b) A referee has requested that, in view of the implications of ref 9a, we provide additional details regarding the construction of Figure 1 and its 3-21G counterpart. In the case of the AM1 surface, we located a structure close to **2** following an initial two-dimensional grid search; this structure was then optimized by using the SIGMA option of AMPAC, which allows the minimization of the gradient norm with respect to the internal coordinates. As can be seen upon inspection of Figure 1, the transition structure **2** would be found as the minimum point of the line, drawn along the ridge of the surface, which joins the "transition states" of the cross sections corresponding to fixed values of r. Each of the points along the ridge had been located approximately during the initial grid search, refined with the SIGMA option, and found to have only one negative eigenvalue in its second derivative matrix. Because these are not saddle points of the full surface, this kind of characterization does not constitute a vibrational analysis; nevertheless, the procedure is valid for the location and characterization of a cross section of the surface, whose maximum corresponds to a transition structure containing one fixed variable. In the cases of the ab initio surfaces, we used the OPT=TS option of GAUSSIAN 86 to find the points along the ridge that correspond to fixed values of r; again, each of these points was found to possess one negative eigenvalue in its second derivative matrix. Since the true transition state **2**, as already noted, is the minimum of the line drawn through these points, by determination whether an increase or decrease in r leads to an increase or decrease in the energy of the ridge point, it was possible without difficulty to reach a structure close to that of **2**. At this stage, all geometrical constraints were released, and, with the aid of the previously calculated Hessian matrix, the final optimization was performed.

(10) Bordwell, F. G.; Hughes, D. L. *J. Org. Chem.* **1982**, *47*, 3224, and references cited therein. Bordwell, F. G.; Hughes, D. L. *J. Am. Chem. Soc.* **1985**, *107*, 4737. Jencks, W. P. *Bull. Soc. Chim.* **1988**, No. 2, 218.

perimental studies of this issue suffer from the disadvantages of the scatter of data points as well as the relatively narrow range in ΔpK_a that is normally dictated by the necessary confinement to a single family of reactants. These limitations are absent from the present theoretical study. Plots of $\Delta E^{\ddagger}$ versus ΔE for the cross sections of the four surfaces ("coupled" and "uncoupled", AM1 and 3-21G) are *linear* in each case, with correlation coefficients 0.998–0.999, over a range of up to 80 kcal/mol in ΔE.[11] Figure 2 shows two of these plots.

Linearity of a Brönsted plot is normally considered to reflect a transition state of constant structure, but, in the present cases, neither the positions of the heavy atoms nor those of the transferred proton are maintained from one cross section to another. Inspection of Figure 1 shows clearly that the transition states for the horizontal movement become more reactant-like as the process becomes more exoergic, in harmony with the BEMA HAPOTHLE.[12] Other indices for transition state location such as O–H bond order[13] and the Miller equation,[14] also show transition states of highly variable structure.

(ii) Use of the Marcus equation (eq 4)[15] and the intrinsic barriers given in Table I reproduces $\Delta E^{\ddagger}$ for the proton-transfer reactions, with deviations ranging from −2.1 to +3.5 kcal/mol, for three of the four surfaces.[16]

$$\Delta E^{\ddagger} = \Delta E^{\ddagger}_0(1 + \Delta E/4\Delta E_0^{\ddagger})^2 \qquad (4)$$

The success of this equation in predicting the activation energies seemed at first to result from the large intrinsic barriers, which reduce the contribution of the quadratic term. However, more detailed statistical analyses of the Brönsted and Marcus treatments lead to a different conclusion. For plot (b) of Figure 2, the correlation coefficient $r = 0.9991$ would be considered excellent, but the relationship between $\Delta E^{\ddagger}$ and ΔE seems to be curved when the plot is examined visually. On the other hand, for the same set of data, Marcus theory with an intrinsic barrier of 22.2 kcal/mol predicts the activation energies reasonably well, as expected[17] for variable transition states.

Which analysis, Marcus or Brönsted, is superior in this case? The quantitative criterion for data fitting is based on the sum of the squares of the deviations divided by the number of degrees of freedom ($\Sigma s^2/df$).[18] Applying this statistical procedure to the data of plot (b) of Figure 2 leads to a fit of 0.58 to the linear treatment, one order of magnitude better than the fit (5.53) to the quadratic treatment.

Since we thus observe (a) linear Brönsted plots whose slopes cannot be interpreted in terms of constant transition-state structure and (b) a correlation with the Marcus equation, indicative of a variable transition state, that is statistically less significant than (a), we conclude that the ubiquitous Brönsted relationship is not yet understood fully and must contain undiscovered mechanistic information.[19]

(iii) In the classical Eigen plot for proton-transfer reactions,[20] the slope is unity for $\Delta pK_a < 0$ and zero for $\Delta pK_a > 0$, in contrast to the results seen in Figure 2. The Eigen plot describes proton transfer between two heteroatoms in solution, and, when $\Delta pK_a > 0$, the transfer of the proton along the hydrogen bond has a smaller barrier than the diffusion barrier. In the gas phase, however, there is no diffusion-controlled upper limit to reaction rates; significant barriers exist and lead to slopes that are different from unity.

(iv) Because of the high barriers, the proton jump hypothesis fails.[3] If the hypothesis were valid for the $H_2O + CH_2O$ reaction, the horizontal cross section of the surface which passes through **2** ($r = 1.53$ Å for AM1 and 1.68 Å for 3-21G) would correspond to the intrinsic barrier for the process, i.e., ΔE ($\equiv\Delta pK_a$) = 0. In fact, in this cross section, the ΔE's are −40 and −29 kcal/mol, respectively, and the intrinsic barriers are found near $r = 1.8$ Å. It follows that the proton jump hypothesis should be restricted mainly to reactions in solution, for which the transfer has a much lower barrier.

It should be noted, finally, that the semiempirical and ab initio results of the present work are in very good agreement, especially for the slopes of the Brönsted plots. In view of its speed and relative simplicity, AM1 appears to be a useful procedure for the evaluation of certain postulates of physical organic chemistry.

Acknowledgment. We thank the Natural Sciences and Engineering Research Council of Canada for financial support and an International Scientific Exchange Award, Professor M. J. S. Dewar for a copy of AMPAC (Version 2.10, VAX), Dr. D. G. Watts for the statistical analyses, and Queen's University for their generous allocation of computer time.

Registry No. CH_2O, 50-00-0.

(11) MNDO calculations of proton transfer between substituted ethanols (Anhede, B.; Bergman, N.-A.; Kresge, A. J. *Can. J. Chem.* **1986**, *64*, 1173) gave a slightly curved Brönsted plot. A slope of ca. 0.4 was obtained in a similar plot for proton transfer from $R_1R_2O^+H$ to H_2O at the 4-31G level. See: Scheiner, S. *Acc. Chem. Res.* **1985**, *18*, 174.

(12) Jencks, W. P. *Chem. Rev.* **1985**, *85*, 511.

(13) Pauling, L. *J. Am. Chem. Soc.* **1947**, *69*, 542.

(14) Miller, A. R. *J. Am. Chem. Soc.* **1978**, *100*, 1984.

(15) Marcus, R. A. *Annu. Rev. Phys. Chem.* **1964**, *15*, 155.

(16) For the "uncoupled" surface calculated at the 3-21G level, deviations as large as 15 kcal/mol are found in the application of eq 4 to the data.

(17) Donnella, J.; Murdoch, J. R. *J. Am. Chem. Soc.* **1984**, *106*, 4724. Agmon, N. *Int. J. Chem. Kinet.* **1977**, *45*, 343.

(18) Mandel, J. *The Statistical Analysis of Experimental Data*; Interscience Publishers: New York, 1964.

(19) Yamataka, H.; Nagase, S. *J. Org. Chem.* **1988**, *53*, 3232.

(20) Eigen, M. *Angew. Chem., Int. Ed. Engl.* **1964**, *3*, 1.